Influence of the Amyloid Dye Congo Red on Curli, Cellulose, and the Extracellular Matrix in *E. coli* during Growth and Matrix Purification

Courtney Reichhardt, Oscar A. McCrate, Xiaoxue Zhou, Jessica Lee, Wiriya Thongsomboon, and Lynette Cegelski*

Stanford University, Department of Chemistry, 380 Roth Way, Stanford CA 94305

*Corresponding author

Contact information: cegelski@stanford.edu, telephone: 650-725-3527, fax: 650-723-4817

Keywords: bacterial biofilm, curli, cellulose, *E. coli*, extracellular matrix, Congo red, CPMAS

ABSTRACT

Microbial biofilms are communities of cells characterized by a hallmark extracellular matrix (ECM) that confers functional attributes to the community including enhanced cohesion, adherence to surfaces, and resistance to external stresses. Understanding the composition and properties of the biofilm ECM is crucial to understanding how it functions and protects cells. New methods to isolate and characterize ECM are emerging for different biofilm systems. Solid-state nuclear magnetic resonance was used to quantitatively track the isolation of the insoluble ECM from the uropathogenic *E. coli* strain UTI89 and understand the role of Congo red in purification protocols. UTI89 assembles amyloid-integrated biofilms when grown on YESCA nutrient agar. The ECM contains curli amyloid fibers and a modified form of cellulose. Biofilms formed by UTI89 and other *E. coli* and *Salmonella* strains are often grown in the presence of Congo red to visually emphasize wrinkled agar morphologies and to score the production of ECM. Congo red is a hallmark amyloid-binding dye and binds to curli, yet also binds to cellulose. We found that growth in Congo red enables more facile extraction of the ECM from UTI89 biofilms and facilitates isolation of cellulose from the curli mutant, UTI89Δ*csgA*. Yet, Congo red has no influence on the isolation of curli from curli-producing cells that do not produce cellulose. Sodium dodecyl sulfate can remove Congo red from curli, but not from cellulose. Thus, Congo red binds strongly to cellulose and possibly weakens cellulose interactions with the cell surface, enabling more complete removal of the ECM. The use of Congo red as an extracellular matrix purification aid may be applied broadly to other organisms that assemble extracellular amyloid or cellulosic materials.

INTRODUCTION

Bacterial biofilms are complex multicellular bacterial communities surrounded by an extracellular matrix (ECM) that confers protection to environmental stress such as desiccation and enhances bacterial resistance to antibiotics and host defenses [1-4]. Although bacteria and microbial fungi have traditionally been studied extensively as planktonic organisms, grown in flasks, microorganisms most often grow as biofilms in native environments. The formation of bacterial biofilms also contributes to serious and persistent human infections such as chronic lung infections, biofouling of medical implants, and urinary tract infections (UTI) [5-10]. A defining feature of a biofilm is the ECM, which is a self-produced and often complex and heterogeneous material that surrounds and protects the associated microorganisms. Typically, ECM is rich in biopolymers and can contain proteins, polysaccharides, lipids, nucleic acids, and other molecules. The ECM is often insoluble and difficult to isolate from the cells in the community, posing major challenges to the identification and quantitative annotation of matrix parts [11,12]. Thus, the complete ECM composition of many biofilm-formers is unknown, and the composition can vary across species and even growth conditions. We have been developing integrated approaches using solid-state NMR spectroscopy together with microscopy and biochemical analyses to provide quantitative compositional descriptions of the extracellular matrix of microbial biofilms, including those formed by *E. coli*, *Vibrio cholerae*, and *Aspergillus fumigatus* [13-16].

The first contribution utilizing this solid-state NMR approach defined the composition of the insoluble ECM formed by the biofilm-forming uropathogenic *E. coli* strain UTI89 [13]. Solid-state NMR measurements of the intact ECM together with spectra of two known ECM parts, an amyloid fiber termed curli and a cellulosic polymer, revealed that the insoluble ECM

material was comprised of only these two components [13]. The major measurements employed one-dimensional solid-state NMR spectroscopy to obtain cross-polarization magic angle spinning (CPMAS) spectra and allowed a complete accounting of the matrix parts. CPMAS can be used to quantify the number of spins at corresponding chemical shifts relative to others in a spectrum, and quantification using CPMAS has been used to characterize a range of systems in addition to the biofilm systems we have examined. Examples include determinations of: the ratio of α- and β-forms of sugars [17] and the extent of cross-links in plant cell walls [18] and bacteria, including *Staphylococcus aureus* [19]. Furthermore, we discovered that the polysaccharide produced by *E. coli* in the ECM was a modified form of cellulose [13]. Double resonance NMR experiments were employed in this determination to identify carbons that were coupled to nitrogen and lead to the determination that the some of the glucose units in cellulose contained ethanolamine substituents. This cellulosic material can be readily isolated from a curli mutant and, as such, is non-crystalline and semi-soluble, in contrast to standard cellulose, which is crystalline and insoluble. Typical microbial cellulose isolation procedures entail harsh treatments with either strong acids or bases followed by mass spectrometry or other solution-based analyses to detect the presence of glucose units [20-22]. Such processing can result in hydrolysis and degradation of ECM material and, in UTI89, also failed to solubilize most of the cellulosic material, which may explain why the cellulose modification had eluded discovery until the solid-state NMR analysis of the intact material.

The ability to isolate and quantitatively study ECM that contains amyloids and/or cellulose, such as UTI89 ECM, is crucial due to the prevalence of these biopolymeric components across many species of microorganisms and the roles that these components play in microbial adhesion to biotic and abiotic surfaces and in biofilm production [11,23]. The

discovery of curli as amyloid in 2002 served as the first identification of a functional bacterial amyloid fiber and was based on significant β-sheet character as determined by circular dichroism measurements and resistance to proteases and sodium dodecyl sulfate (SDS) [24] as well as the ability of curli to bind the amyloid-binding dyes Congo red (CR0 and thioflavin T [25]. In contrast to the amyloids associated with eukaryotic amyloid diseases including Alzheimer's, Parkinson's, and Huntington's diseases where soluble proteins undergo alternative and undesired protein folding pathways en route to amyloidogenic intermediates and amyloid fibers [26,27], bacteria harbor dedicated molecular machinery to assemble amyloids at their cell surface to promote adhesion [28,29] and biofilm formation [23]. A survey of environmental biofilms revealed that amyloid producers are phylogenetically diverse with members of Actinobacteria, Bacteroidetes, Firmicutes, and Gammaproteobacteria able to produce amyloids [30,31]. Additionally, homologous genes for the curli amyloid system have been found across four phyla, although only a few bacterial functional amyloid systems have been well characterized: curli/tafi produced by *E. coli* [32,33]/*Salmonella* spp. [34,35]; chaplins produced by *Streptomyces coelicolor* [36,37]; TasA fibers produced by *Bacillus subtilis* [38]; and FapC fibers produced by *Pseudomonas fluorescens* [39]. Similarly, cellulose is a major molecular determinant of biofilm formation by *E. coli, Salmonella* [35,40,41], and *Pseudomonas* species [42] as well as several other gram-negative and gram-positive bacteria [12]. We note that these cellulose determinations, however, were made using solution-based assays with the caveats described above. Thus, it is possible that cellulose modifications have eluded detection and may also be present in the ECM of these organisms.

Both UTI89 ECM components, curli and cellulose, can bind to the dye Congo red (CR), and in the debut compositional study, UTI89 ECM samples were prepared from cells grown in CR-supplemented YESCA agar medium [13]. For the determination of UTI89 ECM composition, CR was included in the growth medium because the dye was qualitatively useful to track the ECM isolation. Growth in CR did not alter the macroscopic agar-based biofilm morphology of UTI89 or the microstructure observed in electron micrographs. Indeed, CR has not been reported to alter *E. coli* phenotypes [43]. CR has been used extensively in microbial studies of many bacteria [40,41,43,44] and yeast [45,46] as qualitative indicators of various matrix components, including cellulose, amyloid fibers, and other unidentified materials associated with phenotypic variations.

Although CR has been used in many microbiological studies to qualitatively score the production of curli as well as cellulose and other polysaccharides in *E. coli, Salmonella,* and other microbial species [40,41,44], this study is the first in-depth analysis of the use of the dye CR to isolate ECM components and the first quantitative comparison of CR binding to insoluble ECM material *in situ*. Here, we provide direct comparisons of agar morphologies, electron micrographs, and compositional data that reveal clear distinctions in the interactions of CR with curli and cellulose. We also demonstrated that CR facilitates isolation of cellulose and the integrated cellulose-curli matrix material from whole cells. Furthermore, the ECM extraction procedure applied here for UTI89 *E.coli* should be broadly applicable to other organisms due to the prevalence of amyloid and cellulose as ECM components of many species.

MATERIALS AND METHODS

Growth of *E. coli* and ECM extraction protocols

UTI89 ECM, UTI89Δ*csgA* ECM, and MC4100 curli samples for NMR were prepared using variations of the protocol developed by McCrate et al [13]. Briefly, ECM and curli samples were prepared from bacteria grown on YESCA (Yeast Extract/Casamino Acids) agar at 26°C for 60 hours, and CR (25 μg/mL) was included in the agar medium when indicated. Bacteria were harvested into ice cold 10 mM Tris buffer, pH 7.4, and sheared using an OmniMixer Homogenizer (Omni International) on ice (using motor setting 9) for five cycles of 1 min shear and 2 min rest. Cells were removed by centrifuging twice for 10 min at 5000 *g*. For UTI89, but not UTI89*ΔcsgA* or MC4100, cells were subjected to a second round of shearing and centrifugation. When indicated, CR (25 μg/mL) was spiked into the resulting supernatant. Next, the supernatant was spiked with 5 M NaCl to achieve a final concentration of 170 mM and pelleted for 1 h at 13,000 *g*. For non-SDS-washed samples, pellets were resuspended in 10 mM Tris, pH 7.4, incubated overnight at 4 °C, and then pelleted, washed again in Tris buffer, and pelleted at 30,000 *g* for 30 min. For SDS-washed samples, pellets were resuspended in 10 mM Tris, pH 7.4, spiked with a 10% SDS stock to a final concentration of 4% SDS, and incubated, rocking at room temperature overnight. The ECM or curli was then pelleted for 1 h at 13,000 *g*, resuspended in Tris buffer, and pelleted at 30,000 *g* for 30 min. The latter washing step was repeated until the SDS was removed. For extracellular samples that were collected without selective CR precipitation, no CR was included in the growth medium nor was it spiked in during the prep. The supernatant, which contained the extracellular material, was collected after shearing and cell removal, and then the resulting supernatant was dialyzed against distilled water

for 2 days using 100 kD molecular weight cut-off dialysis membrane. All NMR samples were flash frozen in liquid nitrogen and lyophilized. The agar colony morphology assay was initiated by dropping 10 mL of an overnight bacterial culture grown at 37 °C onto YESCA agar medium, either with or without supplementation with CR (25 μg/mL) and incubated at 26 °C for 60 hours.

Solid-state NMR

The solid-state NMR experiments were performed using an 89-mm wide-bore Varian magnet at 11.7 T (499.12 MHz for ^{1}H and 125.52 MHz for ^{13}C) and a home-built four-frequency transmission-line probe with a 13.66 mm long, 6 mm inner-diameter sample coil and a Revolution NMR MAS Vespel stator. Samples were spun in thin-wall 5 mm outer-diameter zirconia rotors (Revolution NMR, LLC) at 7143 Hz, using a Varian MAS control unit. For all NMR experiments, π-pulse lengths were 7 μs for ^{1}H and 10 μs for ^{13}C, and the recycle delay was 2s. Proton-carbon cross-polarization occurred at 50 kHz for 1.5 ms. Proton dipolar coupling was performed at 90 kHz with TPPM modulation. The ^{13}C spectra were referenced to TMS, which was determined relative to an adamantane standard.

Transmission electron microscopy

Negative staining transmission electron microscopy (TEM) was performed on bacterial samples harvested into 10 mM Tris buffer, pH 7.4, after growth on YESCA agar at 26°C for 60 h. Samples were applied to 300-mesh copper grids coated with Formvar film (Electron Microscopy Sciences, Hatfield, PA) for 2 min and then rinsed in deionized water. The samples were negatively stained with 2% uranyl acetate for 90 s, excess stain was wicked off with filter paper, and then the sample was air-dried. Microscopy was performed on the JEM-1400 (JEOL, LLC).

RESULTS AND DISCUSSION

Influence of Congo red during curli production and SDS washing during purification

Curli are typically purified from the MC4100 strain of *E. coli* that produces only curli as extracellular structures. Notably, MC4100 does not produce cellulose, type 1 pili, or flagella. CR is commonly used as an indicator of curli production by MC4100, whereas MC4100 mutants lacking curli do not bind CR. We determined here that CR had no influence on the MC4100 colony morphology or apparent curli structure as observed by TEM (Figure 1A). Solid-state ^{13}C CPMAS NMR spectra of three curli samples were compared to examine the potential influence of CR in NMR spectra of curli and to assess the effect of SDS washing on curli-bound CR. One curli sample was prepared from bacteria grown on standard YESCA agar medium without CR supplementation. Two samples were prepared from bacteria grown on CR-supplemented YESCA agar, where one was treated with SDS after fiber purification and the other was not. The two spectra of curli isolated from SDS-treated cells grown either with CR or without CR were identical, indicating that SDS removed CR from curli fibers (Figure 1B). Samples also lost their red appearance after SDS treatment. The spectra contained only curli protein peaks (carbonyls, aromatics, alpha carbons, and other aliphatics corresponding to the curli monomer, CsgA, sequence) without any detectable NMR signal from CR (Figures 1B and 1C, Table 1). Bound CR would be readily detected in the spectrum if present at or above an amount of 5% by mass, as illustrated in Figure S1, which provides spectral comparisons of different CR-curli sample compositions.

The ^{13}C CPMAS spectrum of curli extracted from cells grown on CR-supplemented agar but without SDS-treatment, contained the additional spectral contributions from CR as evidenced by the increased peak intensities at 128, 152, and 185 ppm (Figures 1D, black spectrum),

consistent with the ability of curli as amyloid fibers to bind CR. The relative contributions from curli and CR were also determined. For this determination, mass-normalized spectra of pure curli, "curli, no CR (+SDS)," and of "CR" were scaled and summed to recapitulate the "curli, CR_{grown} (no SDS)" spectrum (Table 1 and Figure S1). The "curli, CR_{grown} (no SDS)" sample contained approximately 22% CR by mass.

Influence of CR on polysaccharide preparations from the curli mutant, UTI89Δ*csgA*

Isolation of the cellulosic polysaccharide was attempted using the cellulose-producing but curli-deficient strain, UTI89Δ*csgA*, following the same protocols as used above for the preparation of curli from MC4100. In contrast to curli, which could be collected by centrifugation even in the absence of CR ("curli, no CR (+SDS)" sample), no recoverable extracellular material was recovered from UTI89Δ*csgA* if CR was omitted from the centrifugation-based purification protocol. We hypothesized that the cellulosic material was soluble and not collected by centrifugation in the absence of CR, whereas the presence of CR could aid in its precipitation, consistent with previous uses of CR to aid in the precipitation of β-glucans [47]. Thus, we tested whether the simple addition of CR to the cell-homogenized supernatant (after the low-speed removal of intact cells) would be sufficient to aid in the precipitation of the cellulosic material even when no CR was included in the growth medium and biofilm homogenization protocol. Indeed, this exogenous addition of CR before the last and higher speed centrifugation step to collect the extracellular material enabled precipitation of the UTI89Δ*csgA* extracellular material, where this sample is later referred to as "CR_{spike}" to identify it as having had CR spiked in after the homogenization step and to distinguish it from the "CR_{grown}" sample which was prepared from cells grown in the presence of CR. Interestingly, there was a difference observed in the agar

colony morphology of cells grown in the presence of CR: UTI89Δ*csgA* communities adopted a more highly wrinkled morphology when grown on CR-supplemented agar (Figure 2A). By electron microscopy, the extracellular material also appeared to be more tightly bundled (Figure 2A).

To examine if CR affected the composition of UTI89Δ*csgA* ECM, samples were prepared from cells grown with and without CR. When grown in the absence of CR, the cellulose-containing material was isolated from the cells and then precipitated by the addition of CR to the soluble material (at a final CR concentration of 25 μg/mL), presented in Figure 2B as "UTI89Δ*csgA*, CR_{spike} (+SDS)." The resulting spectrum contained contributions from CR (128, 152, and 185 ppm) and cellulose carbons, as well as a 40-ppm carbon ascribed to an ethanolamine modification of cellulose as described previously [13]. Production of the UTI89Δ*csgA* ECM by cells grown in the presence of CR, "UTI89Δ*csgA*, CR_{grown} (+SDS)," had only minor effects on the NMR spectrum (Figure 2B). Both of these samples were treated with SDS and reveal that SDS treatment did not remove CR from cellulose. To determine the amount of CR in each sample, the mass-normalized spectrum of pure CR was scaled to fit the CR contributions (peaks at 128, 152, and 185 ppm) in the UTI89Δ*csgA* ECM spectra (Figure S2). The mass percent of CR was 50% in the "UTI89Δ*csgA*, CR_{grown} (+SDS)" sample and was 48% in the "UTI89Δ*csgA*, CR_{spike} (+SDS)" sample. The potential influence of SDS washing was tested and the NMR spectra revealed that there was very little effect on the UTI89Δ*csgA* ECM spectrum other than to remove a small but detectable amount of CR, illustrated in Figure 2C and with quantification by integrals in Table 1. The non-SDS-treated CR_{grown} sample contained 51% CR as compared to 50% in its SDS-treated counterpart described just above. Thus, unlike curli, SDS is generally unable to appreciably remove the CR that is bound to cellulose. Cellulose is

also able to bind more CR per mass of polymer (50% by mass) than curli which binds CR to an extent of 22% of the curli dry mass.

Furthermore, since the cellulose material was soluble when extracted from cells grown in the absence of CR, we also examined the composition of the entire supernatant after low-speed centrifugation to remove cells and dialysis of the cellulose-containing supernatant followed by lyophilization. The sample contained primarily cellulose with small protein contributions released during biofilm homogenization (Figure S3), consistent with FliC from flagella. Flagella were identified in curli-associated biofilms previously by electron microscopy [48] and FliC was specifically identified through protein gel analysis and protein identification in our ECM preparations before SDS treatment [13]. Flagella are produced by cells that are still dividing and found closest to the nutrient agar in an agar-based biofilm [48] and thus are present in the initial ECM extraction. Yet, flagella are not required or incorporated into the insoluble three-dimensional baskets or networks that are observed around *E. coli* and are removed by SDS treatment[48, 13]. Thus, the use of CR during growth or the use of CR as an exogenous precipitation agent added before final centrifugation helps to separate cellulose from proteins released during the ECM extraction.

Influence of Congo red and SDS washing during isolation of UTI89 ECM

Finally, we examined the biofilm-forming strain UTI89 that produces both curli and cellulose in the ECM. Cells exhibited a similar colony morphology and were visually similar by electron microscopy whether grown in the presence or absence of CR (Figure 3A). However, more ECM could be extracted when cells were grown in the presence of CR than when CR was omitted during growth and only spiked in after the homogenization step for the subsequent precipitation

of the material. In the latter case, CR was spiked in to a final CR concentration of 25 μg/mL as above. Typical ECM yields were 35 to 60 mg of UTI89 ECM per L agar medium when CR was included in the growth medium and only 10 to 20 mg of ECM per L agar medium when CR was not present in the nutrient agar and only spiked in for precipitation purposes. In contrast, the extraction of curli from MC4100 or the cellulose material from UTI89Δ*csgA* did not have any dependence on growth with CR, and 15 to 20 mg/L of material were routinely harvested from each whether grown in the presence or absence of CR.

The NMR spectra of UTI89 ECM contained the combined spectral signatures from curli, cellulose, and Congo red. The relative amounts of each constituent depended upon whether CR and SDS were employed in the preparations as indicated in the Figure 3 spectra and tabulated in Table 1. The ECM collected from cells grown in the presence of CR had a curli content of 72%, cellulose content of 14%, and Congo red content of 14% (Figure S5a). This is consistent with previous work in which the cellulose content in the UTI89 ECM extracted from cells grown with CR was reported to range from 12-15% [13]. A replicate sample yielded a nearly identical spectrum, with the spectral overlap provided in Figure S5. When the ECM was isolated from cells grown in the absence of CR, but in which CR was used as the precipitation aid, the cellulose peaks (74, 82, and 103 ppm) were reduced (Figure 3B). The total cellulose content was reduced from 14% ("UTI89 ECM, CR_{grown} (+SDS)") to 10% of the total sample mass (Figure 3B; Figure S4). Together with the decreased yield obtained for ECM extracted from cells grown in the absence of CR, this result is consistent with the hypothesis that CR aids in the extraction of the ECM, particularly the polysaccharide component. Alternatively, it is possible that cellulose production was just reduced in addition to the decreased extraction efficiency in the absence of CR. UTI89 biofilms formed in the presence or absence of CR exhibited similar macroscopic

colony morphologies and were indistinguishable by electron microscopy. Thus, either possibility does not result in obvious changes to the biofilm community.

One additional observation from the collective NMR spectra involves the partial removal of CR during SDS treatment of the UTI89 ECM. As noted above, SDS removed all CR from the curli-only sample, whereas SDS did not appreciably remove CR from the cellulose-only sample. Thus, it was anticipated that SDS would not completely remove CR in the UTI89 ECM sample since it contains cellulose in addition to curli. Indeed, SDS removed only some CR contributions from the spectrum (Figure 3D), where the CR-only spectrum was shown for reference in Figure 1C. The CR that remained bound was likely associated with cellulose.

Finally, given the use of SDS in the preparation of the insoluble ECM from *E. coli* biofilms, we sought to examine the possible effects that SDS could have on matrix architecture. SDS has been included in the ECM isolation in order to remove the small amount of detectable protein contaminants from flagella and cell-membrane associated proteins that are released upon homogenization, but which are not part of the insoluble matrix [13]. Thus, TEM was employed to compare the visual appearance of the SDS-treated and nontreated UTI89 ECM. Major networks of UTI89 ECM remained intact following SDS treatment (Figure 4).

CONCLUSIONS

E. coli, *Salmonella,* and other biofilms are commonly characterized through CR binding phenotypes and agar-based morphology assays [13, 40-46]. We have harnessed the ability of the UTI89 ECM components curli and cellulose to bind CR as an aid in the selective isolation of the ECM from cells in the UTI89 biofilm. We discovered that the ECM extraction efficiency from UTI89 biofilms formed on CR-supplemented agar was greater than when cells were grown

without CR, suggesting that CR may weaken the association of cellulose with the cell surface if present as the matrix components are being secreted and assembled. The ability of CR to interact with the modified cellulose produced by *E. coli* was also evident in experiments performed with the curli mutant, UTI89*ΔcsgA*. CR was required either during the growth or as an additive after the cell harvest to enable precipitation of the cellulose. In either case, cellulose bound an equal mass of Congo red to the cellulose mass. Additionally, when CR was added during the growth, a more compact and dense collection of cellulose fibers enmeshed the cells, consistent with the ability of CR to enable precipitation of the otherwise soluble cellulose fibers. This was even paralleled by macroscopic wrinkling in the drop-plate colony morphology assay. In contrast, no visual differences were observed whether UTI89 biofilms (producing both curli and cellulose) were grown in the presence or absence of CR. Due to our determination that the UTI89 ECM contains curli and cellulose in about a 6:1 ratio, we hypothesize that most of the cellulose in the UTI89 ECM is in contact with curli, leaving CR little ability to impact the packing of cellulose fibers.

Congo red has been a fascinating small molecule in the realm of microbiology and also in the broader amyloid field, commonly used to detect and diagnose the presence of β-amyloid deposits in brain tissue, for example. In these applications, CR is typically employed as a spectator dye and exploited for screening and characterization purposes. Through our work and in a more static snapshot sense, we have employed CR as a precipitation agent and tracked and detailed the presence and contributions of CR in matrix preparations. Yet, we have also observed that CR can be a more active molecular participant when biofilms are formed from cells growing on CR-supplemented nutrient agar. Growth in CR generated more densely packed cellulose fibers around UTI89*ΔcsgA* cells and enhanced the removal of ECM from UTI89, potentially

through weakening ECM interactions with the cell surface. These concepts and protocols applied here for *E.coli* UTI89 will be important in future atomic-level studies to model ECM architecture and should be broadly applicable to other organisms due to the prevalence of amyloid and polysaccharides as ECM components of many species.

Acknowledgements

We gratefully acknowledge support from the NIH Director's New Innovator Award (DP2OD007488), the Stanford Terman Fellowship, and the NSF CAREER Award (1453247). C. R. was the recipient of the Althouse Family Stanford Graduate Student Fellowship.

References

1. Hall-Stoodley L, Costerton JW, Stoodley P. Bacterial biofilms: from the natural environment to infectious diseases. Nat Rev Microbiol. 2004; doi:10.1038/nrmicro821

2. Donlan RM, Costerton JW. Biofilms: survival mechanisms of clinically relevant microorganisms. Clin Microbiol Rev. 2002; doi:10.1128/cmr.15.2.167-193.2002

3. Costerton JW, Stewart PS, Greenberg EP. Bacterial biofilms: A common cause of persistent infections. Science. 1999;284:1318-1322.

4. Watnick P, Kolter R. Biofilm, city of microbes. J Bacteriol. 2000;182:2675-2679.

5. Lam J, Chan R, Lam K, Costerton JW. Production of mucoid microcolonies by *Pseudomonas aeruginosa* within infected lungs in cystic fibrosis. Infect Immun. 1980;28:546-556.

6. Valenza G, Tappe D, Turnwald D, Frosch M, Konig C, Hebestreit H, Abele-Horn M. Prevalence and antimicrobial susceptibility of microorganisms isolated from sputa of patients with cystic fibrosis. Journal of cystic fibrosis. 2008; doi:10.1016/j.jcf.2007.06.006

7. Litzler P-Y, Benard L, Barbier-Frebourg N, Vilain S, Jouenne T, Beucher E, Bunel C, Lemeland J-F, Bessou J-P. Biofilm formation on pyrolytic carbon heart valves: influence of surface free energy, roughness, and bacterial species. The Journal of Thoracic and Cardiovascular Surgery. 2007; doi:10.1016/j.jtcvs.2007.06.013

8. Kudinha T, Johnson JR, Andrew SD, Kong F, Anderson P, Gilbert GL. Genotypic and phenotypic characterization of *Escherichia coli* isolates from children with urinary tract infection and from healthy carriers. The Pediatric Infectious Disease Journal. 2013;doi:10.1097/INF.0b013e31828ba3f1

9. Anderson GG, Palermo JJ, Schilling JD, Roth R, Heuser J, Hultgren SJ. Intracellular bacterial biofilm-like pods in urinary tract infections. Science. 2003;301:105-107.

10. Anderson GG, Dodson KW, Hooton TM, Hultgren SJ. Intracellular bacterial communities of uropathogenic *Escherichia coli* in urinary tract pathogenesis. Trends Microbiol. 2004;doi:10.1016/j.tim.2004.07.005

11. Flemming HC, Wingender J. The biofilm matrix. Nat Rev Microbiol. 2010;doi:10.1038/nrmicro2415

12. Flemming HC, Neu TR, Wozniak DJ. The EPS matrix: the "house of biofilm cells". J Bacteriol. 2007;doi:10.1128/JB.00858-07

13. McCrate OA, Zhou X, Reichhardt C, Cegelski L. Sum of the parts: composition and architecture of the bacterial extracellular matrix. J Mol Biol. 2013;doi:10.1016/j.jmb.2013.06.022

14. Reichhardt C, Ferreira JA, Joubert LM, Clemons KV, Stevens DA, Cegelski L. Analysis of the *Aspergillus fumigatus* biofilm extracellular matrix by solid-state nuclear magnetic resonance spectroscopy. Eukaryot Cell. 2015;doi:10.1128/EC.00050-15

15. Reichhardt C, Fong JC, Yildiz F, Cegelski L. Characterization of the *Vibrio cholerae* extracellular matrix: a top-down solid-state NMR approach. Biochim Biophys Biomembranes. 2015;doi:10.1016/j.bbamem.2014.05.030

16. Reichhardt C, Cegelski L. Solid-state NMR for bacterial biofilms. Mol Phys. 2014;doi:10.1080/00268976.2013.837983

17. Chen YY, Luo SY, Hung SC, Chan SI, Tzou DL. ^{13}C solid-state NMR chemical shift anisotropy analysis of the anomeric carbon in carbohydrates. Carbohydr Res. 2005;doi:10.1016/j.carres.2005.01.018

18. Cegelski L, O'Connor RD, Stueber D, Singh M, Poliks B, Schaefer J. Plant cell-wall cross-links by REDOR NMR spectroscopy. J Amer Chem Soc. 2010;132:16052-16057.

19. Romaniuk JA, Cegelski L. Bacterial cell wall composition and the influence of antibiotics by cell-wall and whole-cell NMR. Philosophical transactions of the Royal Society of London Series B, Biological sciences. 2015;doi:10.1098/rstb.2015.0024

20. Decho AW, Visscher PT, Reid PP. Production and cycling of natural microbial extracellular polymers (EPS) within a marine stromatolite. Paleogeogr Paleoclimat Paleoecol 2005;219:71-88.

21. Santos SM, Carbajo JM, Quintana E, Ibarra D, Gomez N, Ladero M, Eugenio ME, Villar JC. Characterization of purified bacterial cellulose focused on its use on paper restoration. Carbohydr polym. 2015;doi:10.1016/j.carbpol.2014.03.064

22. Esa F, Tasirin SM, Rahman NA. Overview of bacterial cellulose production and application. Agriculture and Agricultural Science Procedia 2014;doi:10.1016/j.aaspro.2014.11.017

23. Barnhart MM, Chapman MR. Curli biogenesis and function. Annu Rev Microbiol. 2006;doi:10.1146/annurev.micro.60.080805.142106

24. Manning M, Colon W. Structural basis of protein kinetic stability: Resistance to sodium dodecyl sulfate suggests a central role for rigidity and a bias toward beta-sheet structure. Biochemistry. 2004;doi:10.1021/Bi0491898

25. Chapman MR, Robinson LS, Pinkner JS, Roth R, Heuser J, Hammar M, Normark S, Hultgren SJ. Role of *Escherichia coli* curli operons in directing amyloid fiber formation. Science. 2002;doi:10.1126/science.1067484

26. Chiti F, Dobson CM. Protein misfolding, functional amyloid, and human disease. Annu Rev Biochem. 2006;75:333-366.

27. Cohen FE, Kelly JW. Therapeutic approaches to protein-misfolding diseases. Nature. 2003;426:905-909.

28. Barak JD, Gorski L, Naraghi-Arani P, Charkowski AO. *Salmonella enterica* virulence genes are required for bacterial attachment to plant tissue. Appl Environ Microbiol. 2005;doi:10.1128/AEM.71.10.5685-5691.2005

29. Ryu JH, Kim H, Frank JF, Beuchat LR. Attachment and biofilm formation on stainless steel by *Escherichia coli* O157:H7 as affected by curli production. Letters Appl Microbiol. 2004;doi:10.1111/j.1472-765X.2004.01591.x

30. Larsen P, Nielsen JL, Dueholm MS, Wetzel R, Otzen D, Nielsen PH. Amyloid adhesins are abundant in natural biofilms. Environ Microbiol. 2007;9:3077-3090.

31. Larsen P, Nielsen JL, Otzen D, Nielsen PH. Amyloid-like adhesins produced by floc-forming and filamentous bacteria in activated sludge. Appl Environ Microbiol. 2008;74:1517-1526.

32. Lim JY, Pinkner JS, Cegelski L. Community behavior and amyloid-associated phenotypes among a panel of uropathogenic *E. coli*. Biochem Biophys Res Comm. 2014;doi:10.1016/j.bbrc.2013.11.026

33. Wang X, Smith DR, Jones JW, Chapman MR. *In vitro* polymerization of a functional *Escherichia coli* amyloid protein. J Biol Chem. 2007;doi:10.1074/jbc.M609228200

34. Collinson SK, Emody L, Muller KH, Trust TJ, Kay WW. Purification and characterization of thin, aggregative fimbriae from *Salmonella enteritidis*. J Bacteriol 1991;173:4773-4781.

35. Romling U, Bian Z, Hammar M, Sierralta WD, Normark S. Curli fibers are highly conserved between *Salmonella typhimurium* and *Escherichia coli* with respect to operon structure and regulation. J Bacteriol. 1998;180:722-731.

36. Bokhove M, Claessen D, de Jong W, Dijkhuizen L, Boekema EJ, Oostergetel GT. Chaplins of Streptomyces coelicolor self-assemble into two distinct functional amyloids. J Struct Biol. 2013;doi:10.1016/j.jsb.2013.08.013

37. Capstick DS, Jomaa A, Hanke C, Ortega J, Elliot MA. Dual amyloid domains promote differential functioning of the chaplin proteins during *Streptomyces* aerial morphogenesis. Proc Natl Acad Sci USA. 2011;doi:10.1073/pnas.1018715108

38. Romero D, Aguilar C, Losick R, Kolter R. Amyloid fibers provide structural integrity to *Bacillus subtilis* biofilms. Proc Natl Acad Sci USA. 2010;doi:10.1073/pnas.0910560107

39. Dueholm MS, Petersen SV, Sonderkaer M, Larsen P, Christiansen G, Hein KL, Enghild JJ, Nielsen JL, Nielsen KL, Nielsen PH, Otzen DE. Functional amyloid in *Pseudomonas*. Mol Microbiol. 2010;doi:10.1111/j.1365-2958.2010.07269.x

40. Zogaj X, Nimtz M, Rohde M, Bokranz W, Romling U. The multicellular morphotypes of *Salmonella typhimurium* and *Escherichia coli* produce cellulose as the second component of the extracellular matrix. Mol Microbiol. 2001;39:1452-1463.

41. Zogaj X, Bokranz W, Nimtz M, Romling U. Production of cellulose and curli fimbriae by members of the family Enterobacteriaceae isolated from human gastrointestinal tract. Infect Immun. 2003;71:4151-4158.

42. Ude S, Arnold DL, Moon CD, Timms-Wilson T, Spiers AJ. Biofilm formation and cellulose expression among diverse environmental *Pseudomonas* isolates. Environ Microbiol. 2006;8:1997-2011.

43. Reichhardt C, Jacobson AN, Maher MC, Uang J, McCrate OA, Eckart M, Cegelski L. Congo red interactions with Curli-Producing *E. coli* and Native Curli Amyloid Fibers. PloS ONE. 2015;doi:10.1371/journal.pone.0140388

44. McCrate OA, Zhou X, Cegelski L. Curcumin as an amyloid-indicator dye in *E. coli*. Chem Commun. 2013;doi:10.1039/c2cc37792f

45. Garcia MC, Lee JT, Ramsook CB, Alsteens D, Dufrene YF, Lipke PN. A role for amyloid in cell aggregation and biofilm formation. PLoS ONE. 2011;doi:10.1371/journal.pone.0017632.g001

46. Garcia-Sherman MC, Lundberg T, Sobonya RE, Lipke PN, Klotz SA. A unique biofilm in human deep mycoses: fungal amyloid is bound by host serum amyloid P component. NPJ Biofilms and Microbiomes. 2015;doi:10.1038/npjbiofilms.2015.9

47. Wood PJ, Fulcher RG. Interaction of some dyes with cereal beta-glucans. Cereal Chemistry. 1978;55:952-966.

48. Serra DO, Richter AM, Klauck G, Mika F, Hengge R. Microanatomy at Cellular Resolution and Spatial Order of Physiological Differentiation in a Bacterial Biofilm. mBio 2013;4;e00103-13

Figures

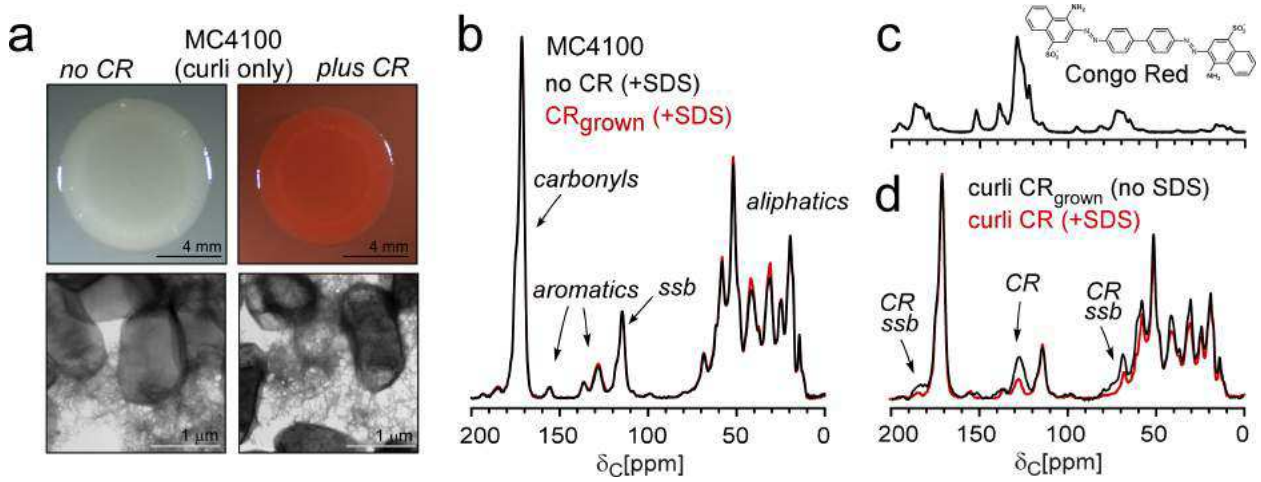

Figure 1. Comparison of curli grown in the presence and absence of Congo red and the influence of SDS washing. (a) MC4100 colony morphology was not altered when grown with CR. As visualized by TEM, CR did not impact the appearance of curliated MC4100 cells. (b) The ^{13}C CPMAS spectrum of SDS-treated curli are comparable whether or not cells were grown in the presence of CR, indicating that most CR was removed in the SDS-treated sample. (c) The ^{13}C CPMAS spectrum of CR is provided as a spectral reference. (d) SDS-treated and non-SDS-treated curli exhibited comparable curli contributions to the NMR spectra, consistent with the ability of amyloids to resist denaturation by SDS treatment. The contributions of CR bound to curli are apparent in the non-SDS-treated sample spectrum (black).

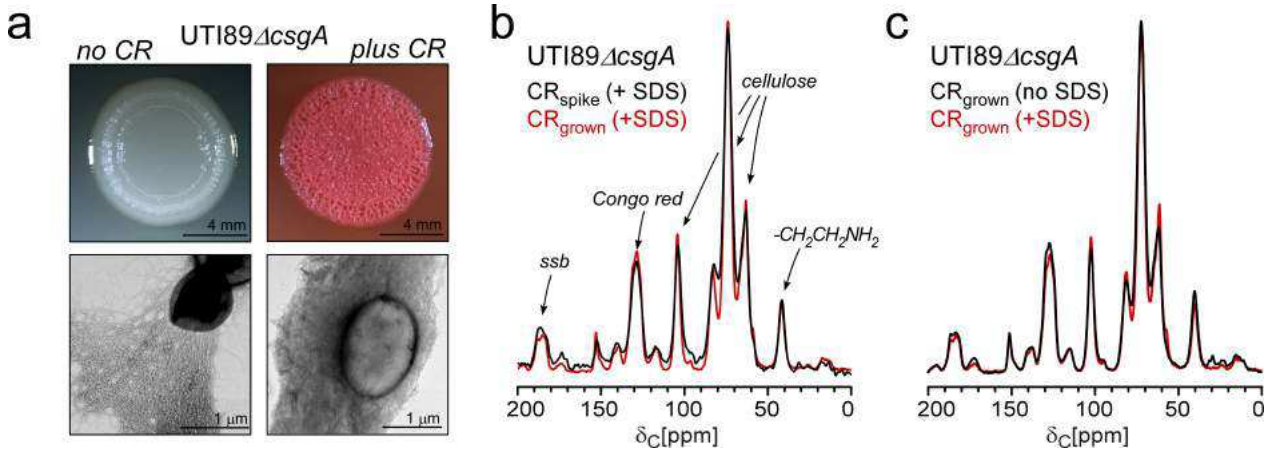

Figure 2. Analysis of UTI89Δ*csgA* polysaccharide samples as a function of Congo red and SDS preparation. (a) CR resulted in some wrinkling of UTI89Δ*csgA.* The extracellular material appeared to be more tightly bundled by TEM. Both growth in CR (b) and treatment with SDS (c) had only minor effects on the ^{13}C CPMAS spectra of UTI89*ΔcsgA* polysaccharide samples.

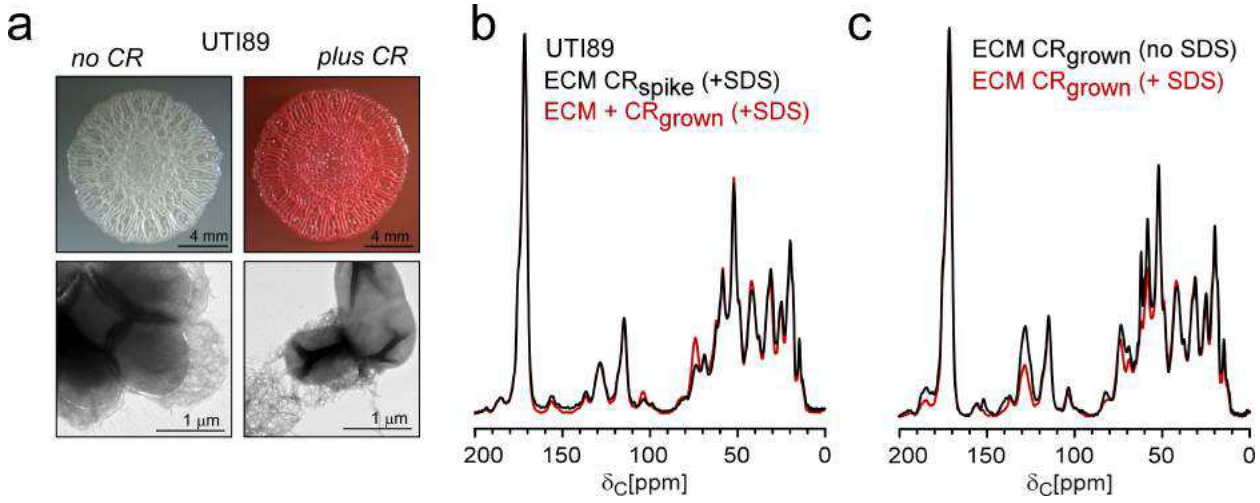

Figure 3. Influence of Congo red and SDS on the UTI89 ECM. (a) Bacterial biofilm formation was visualized macroscopically and microscopically in the presence and absence of Congo red. Biofilms formed by UTI89 on YESCA agar contained both curli and cellulose and exhibited the hallmark wrinkled colony morphology that is accentuated visually in the presence of CR. The colony morphology was similar for cells grown in the presence or absence of CR. Electron microscopy also suggested that the biofilms were similar, and the extracellular baskets previously reported could be identified in samples independent of growth in CR. (b) The ^{13}C CPMAS spectrum of the UTI89 ECM from cells grown in the presence of CR corresponds to 72% curli, 14% cellulose, and 14% CR. Cellulose and CR content in the ECM was lower when CR was only added as a precipitation agent rather than included during growth (black spectrum). (c) SDS-treatment removed some, but not all, CR from UTI89 ECM, consistent with SDS being able to remove CR from curli but not cellulose.

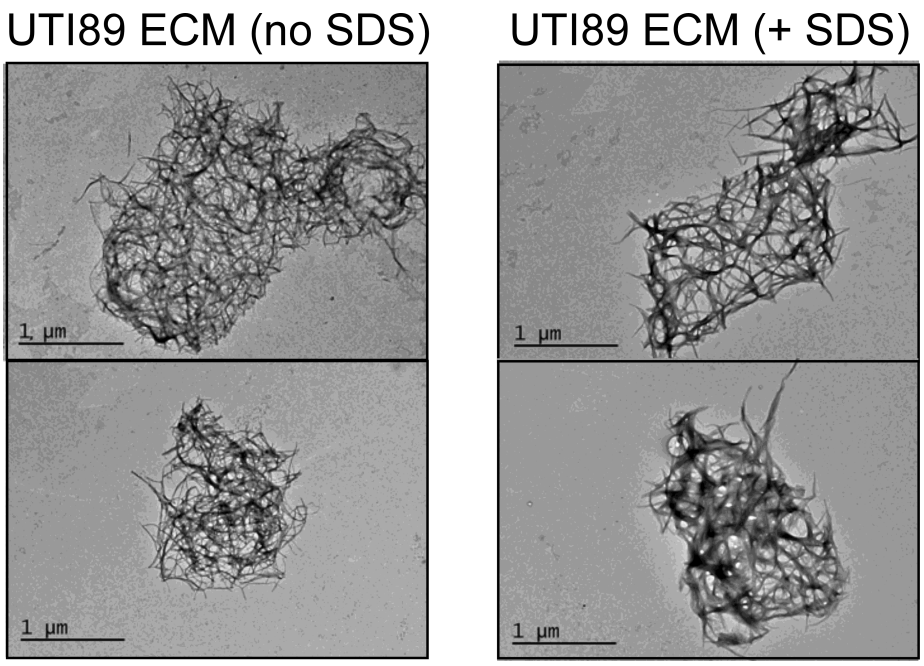

Figure 4. Effect of SDS on UTI89 ECM networks. The TEM images show that SDS does not destroy the major networks observed in the UTI89 ECM.

Influence of the Amyloid Dye Congo Red on Curli, Cellulose, and the Extracellular Matrix in *E. coli* during Growth and Matrix Purification

Courtney Reichhardt, Oscar A. McCrate, Xiaoxue Zhou, Jessica Lee, Wiriya Thongsomboon, and Lynette Cegelski*

SUPPLEMENTAL INFORMATION

Supplemental Figures 1-5

SUPPLEMENTAL FIGURES

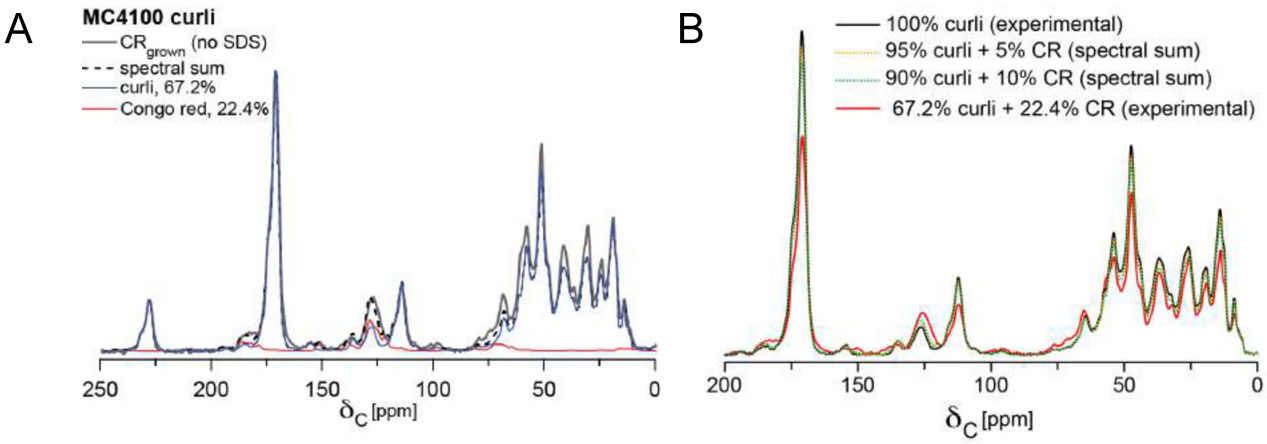

Supplemental Figure 1. (A) The mass normalized spectra of curli and Congo red were scaled by 67.2% and 22.4%, respectively, to recapitulate the spectrum of "Curli, CR_{grown} (no SDS)." The remaining 10.4% of the mass was due to non-curli and non-CR molecules that were not removed by rinsing with Tris buffer. (B) Comparisons of spectral changes expected for samples with varying curli-CR compositions.

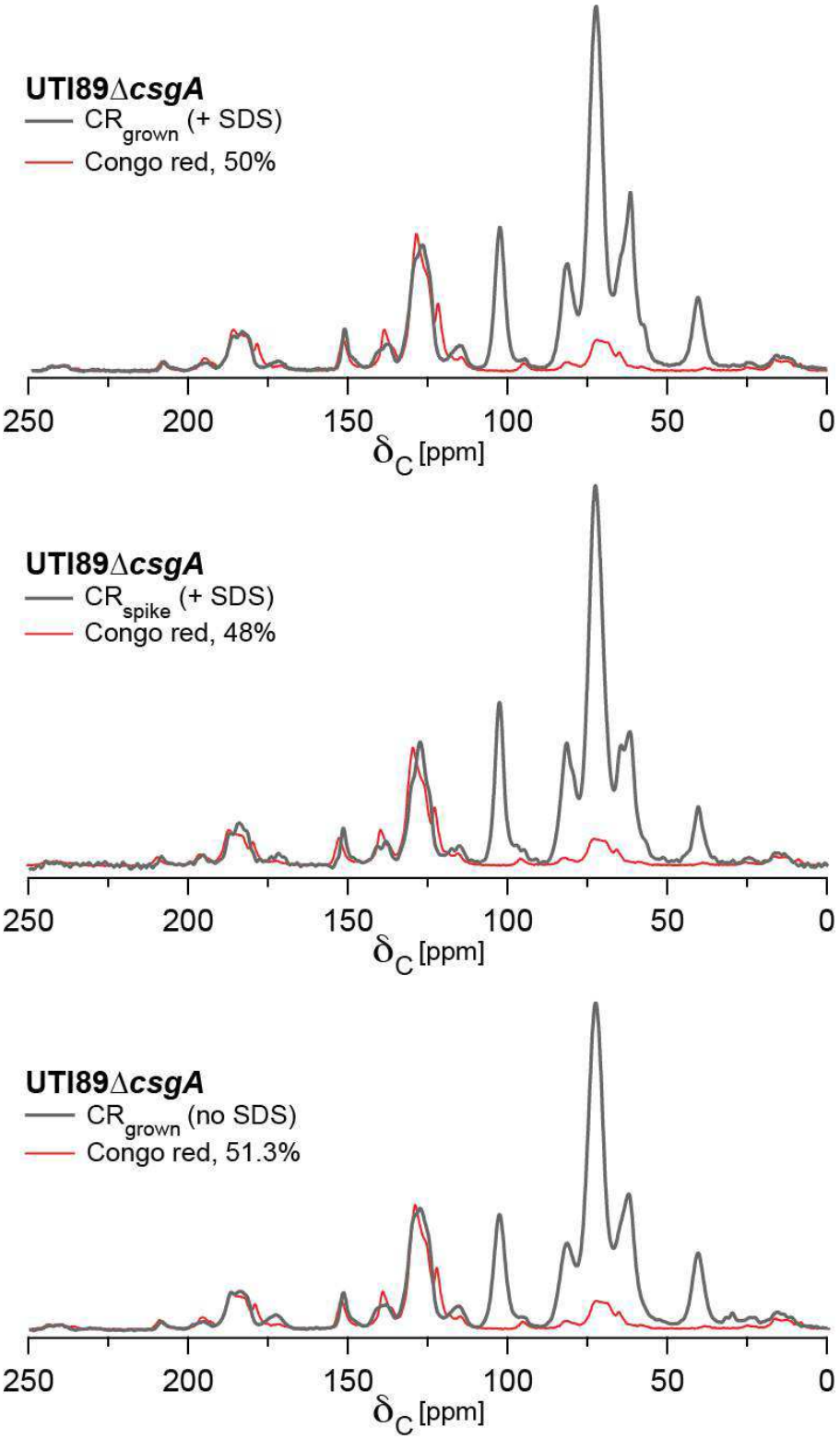

Supplemental Figure 2. The mass normalized spectrum of Congo red was scaled to best fit the spectrally resolved CR peak at 128 ppm in the three UTI89Δ*csgA*-related spectra shown in Figure 2.

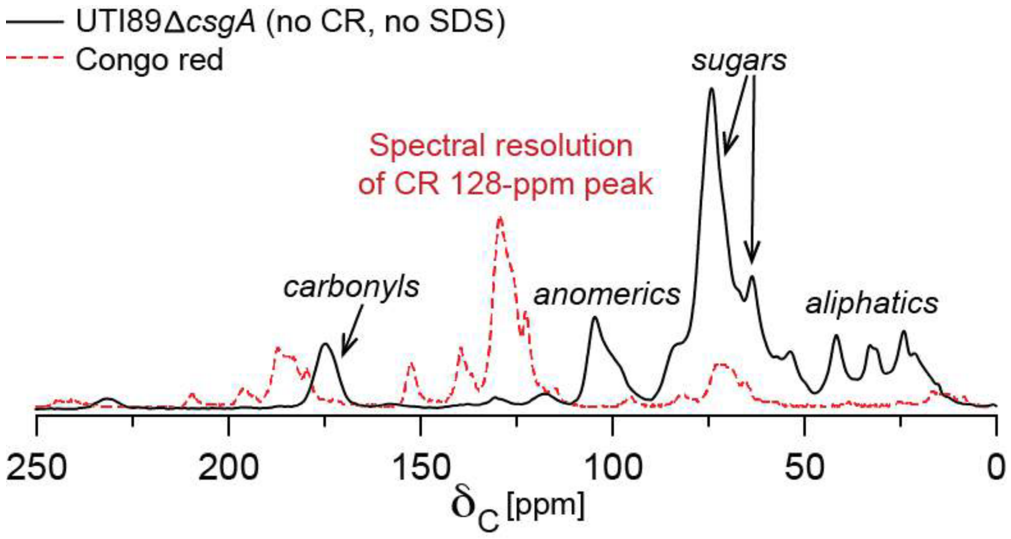

Supplemental Figure 3. UTI89Δ*csgA* extracellular material was isolated without CR precipitation, centrifugation steps, or SDS-washing. This material contained contributions due to soluble proteins that were not part of the insoluble UTI89 ECM. The CR spectrum is shown to highlight the spectral resolution of CR peaks from those of the UTI89 modified cellulose.

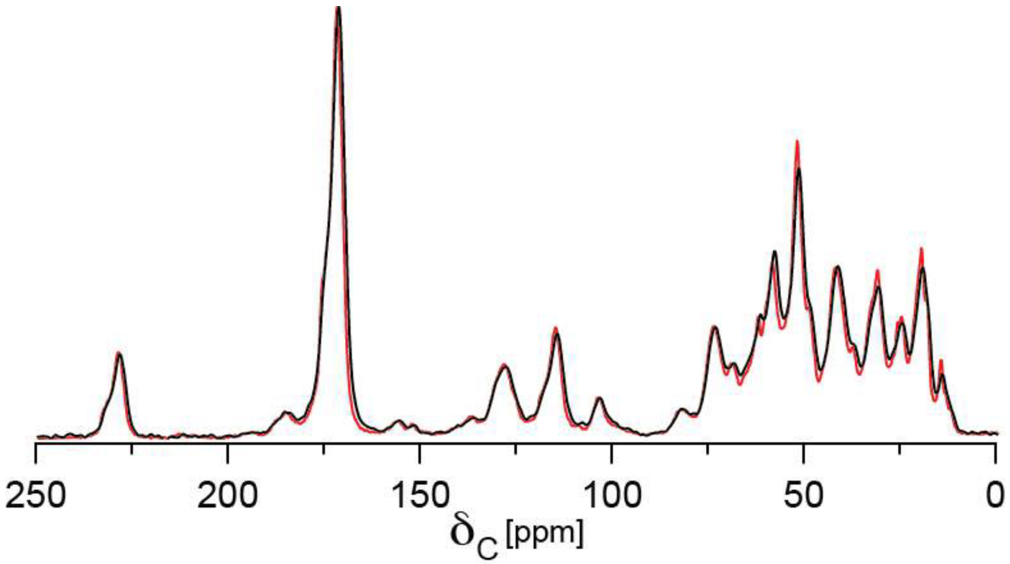

Supplemental Figure 4. Two biological replicates of UTI89 ECM prepared using growth in CR-supplemented agar medium and SDS treatment (prepared by two different researchers two years apart) yielded nearly identical spectra.

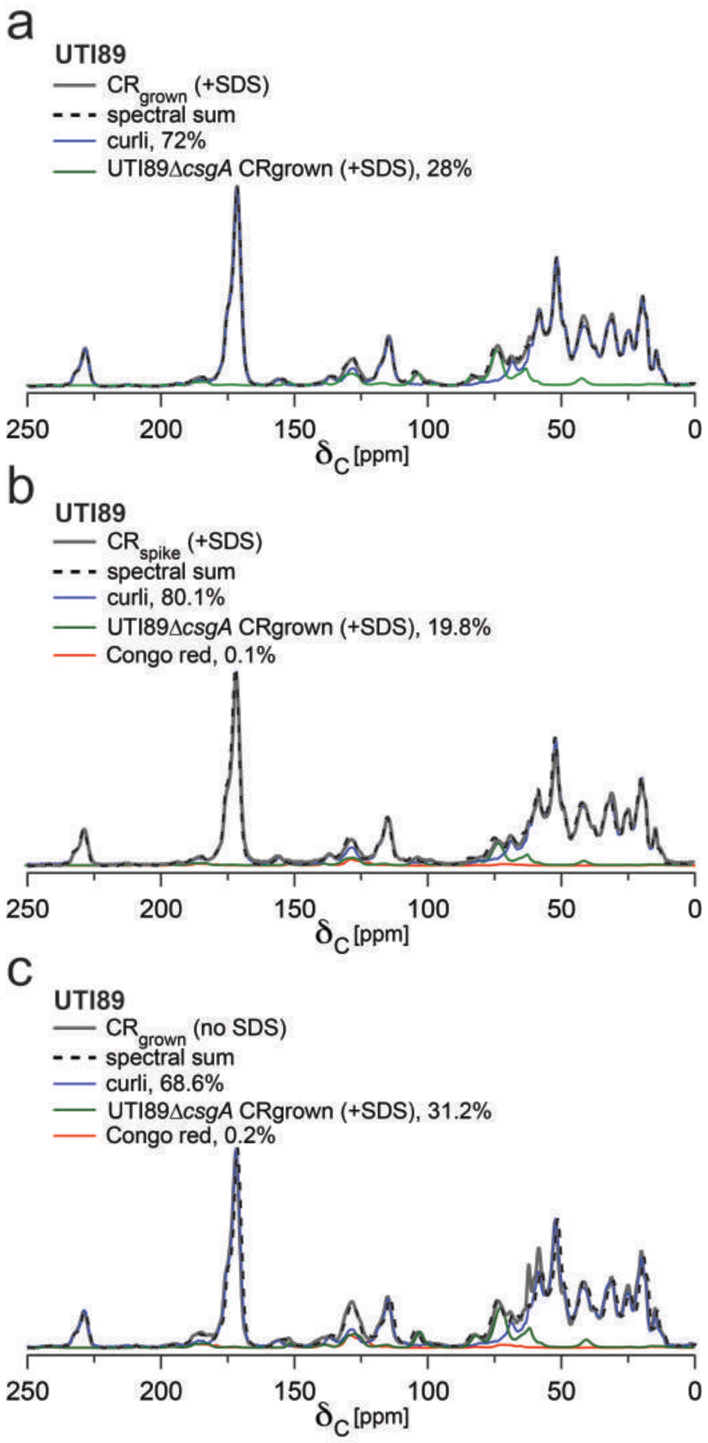

Supplemental Figure 5. The mass normalized spectra of curli, UTI89Δ*csgA* extracellular material, and Congo red were scaled to recapitulate the spectra of UTI89 ECM prepared under varying conditions. The spectrum of UTI89Δ*csgA* extracellular material contains 50% CR and 50% cellulosic material by mass. The CR contributions from the UTI89Δ*csgA* material plus any additional CR were used to determine the total CR mass percentages that were reported in the text.